cis-Bimetalloporphycene

International Edition: DOI: 10.1002/anie.201508409
German Edition: DOI: 10.1002/ange.201508409

β,β′-Bipyrrole Fusion-Driven *cis*-Bimetallic Complexation in Isomeric Porphyrin

*Tridib Sarma, B. Sathish Kumar, and Pradeepta K. Panda**

Dedicated to Professor Varadachari Krishnan

Abstract: *An unprecedented cis-bimetallic complex of dinaphthoporphycene (DNP), namely [Pd_2(μ-DNP)(μ-$OAc)_2$], is reported. The most striking feature of this complex is that two palladiums coordinate to the macrocycle on the same side and are closely held together (Pd–Pd: 2.67 Å) by two bridging acetate ligands exhibiting significant metal–metal bonding interaction (bond order 0.18 evaluated by NBO analysis). Interestingly, replacing acetate with acetylacetonate (acac) could stabilize an unusual mono-palladium complex of DNP, where Pd coordinates unsymmetrically to two ring Ns above the macrocyclic plane, as well as coordinating with two Os of the acac ligand. Remarkably, the rigid DNP core displays enhanced complexation induced aromaticity (as per NICS and HOMA analysis), despite undergoing severe core deformation during complexation with metal ion(s) as noticed from their solid-state structures.*

Metal coordination chemistry of porphyrins is of great interest to researchers.[1] Owing to the smaller core size of the porphyrin macrocycle, it complexes with only one metal ion. On the other hand, bimetallic complexes of porphyrins are very rare and emerged first with the discovery of bis[tricarbonylrhenium(I)] complex of tetraphenylporphyrin (TPP) by Tsutsui.[2] Recently, Boitrel and co-workers reported several bimetallic complexes of functionalized doubly strapped porphyrins, displaying interesting tunable cooperative process and dynamic behavior.[3] Further, Partyka et al. also reported an interesting di-Au^I complex of octaethylporphyrin.[4] These metalloporphyrins exhibit coordination of the two metal ions above and below the porphyrin plane.

Porphycene is an abiotic constitutional isomer of porphyrin, first reported by Vogel and co-workers in 1986, and displays many interesting attributes similar to porphyrins owing to its N4 core.[5] However, owing to its rectangular coordination core and reduced symmetry, it shows enhanced absorption in the red region. This drove the initial applications of porphycene as potential photosensitizers in photodynamic therapy (PDT).[6] It is notable that the β-octasubstituted analogues of porphycene were non-fluorescent, and thus of little utility in PDT.[7] Therefore, very limited attention has been given towards them, including their coordination ability. Recently, Sessler and co-workers reported π-complexes of metalloporphycenes.[8] Very recently, Grill and co-workers demonstrated controlled adsorption of the cis-tautomer of porphycene over a Cu(110) surface.[9] To our knowledge, there is only one sigma bimetallic complex of porphycene so far reported by Che et al., a Re^I complex analogous to that reported by Tsutsui for porphyrins.[10] However, the N4 core of neither porphyrin nor its isomers complexing with two interacting metal ions on the same side of the macrocyclic core is yet to be envisaged. Moreover, it is worth mentioning that most of these bimetallic non-planar complexes of either porphyrin or porphycene are with the larger metal ions of period 6. Remarkably, in all of the Pd^{II} complexes of these ligands, Pd^{II} were found to be inside the N4-core of the macrocycle.

Metalloporphyrinoid studies that reveal, among other things, new metal complexation features are likely to be of both fundamental interest and potential practical utility.[11] Herein, we report a homofacial cis-bimetallic complex of porphycene, that is, a dipalladium complex of dinaphthoporphycene (DNP) **1** with metal–metal bonding interactions. We also report another unsymmetrically coordinated mono-Pd^{II} complex of DNP that forms upon changing the counter anion of the metal salt from acetate to acetylacetonate (acac), as well as the reaction conditions, wherein the porphycene acts as a bidentate ligand without any protection. In both of these cases, the Pd ion sits above the macrocyclic core. Both complexes were characterized by single crystal X-ray structural analysis as well as their optical and electrochemical properties were evaluated.

Vogel and co-workers demonstrated that the geometry of the porphycene core is largely dependent upon its peripheral substitution pattern, and thus the N4-coordination core can be sterically modulated (Figure 1).[7b] In this regard, β-octaalkylporphycenes (such as **4**) possess the most square-type core as well as weak NH···N hydrogen bonding interactions, and are therefore proposed as better ligands.[7a] On the other hand, *meso*-tetrasubstituted porphycenes (**2**) display strong NH···N hydrogen bonds along with a distinct rectangular core, and thus are harder to complex as their lone pairs on nitrogen are not properly oriented towards the metal center.[7c,12] The coordination properties of these *meso*-tetrasubstituted porphycenes has hardly been explored in detail. Recently we found that DNP, wherein two naphthalene units are fused with the opposite bipyrroles, lies at the

[*] Dr. T. Sarma, B. S. Kumar, Dr. P. K. Panda
School of Chemistry, University of Hyderabad
Hyderabad-500046 (India)
E-mail: pkpsc@uohyd.ernet.in
pradeepta.panda@gmail.com

Supporting information and ORCID(s) for the author(s) for this article are available on the WWW under http://dx.doi.org/10.1002/anie.201508409.

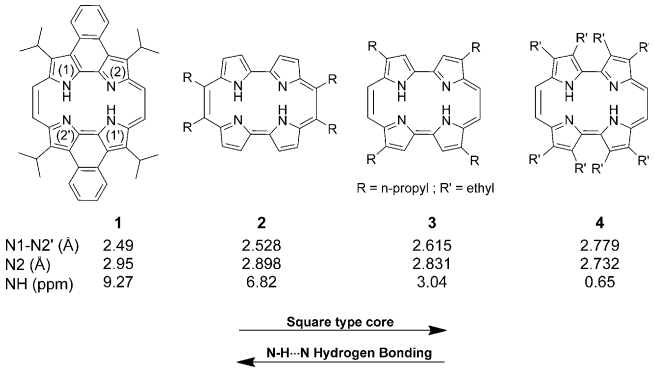

	1	2	3	4
N1-N2′ (Å)	2.49	2.528	2.615	2.779
N2 (Å)	2.95	2.898	2.831	2.732
NH (ppm)	9.27	6.82	3.04	0.65

Figure 1. Variation of core geometry of porphycene with substitution pattern.

extreme end, possessing the most distinct rectangular core as well as the strongest NH···N hydrogen bonding interactions (Figure 1).[13a,b] Our attempt to study the coordination behavior of this presumably poor ligand (because of its rectangular core) revealed that, upon metallation, DNP exhibits an unprecedented near-square N4-core, as inferred from the crystal structure of its Ni^{II} and Cu^{II} complexes (N1–N2: 2.64 Å, N1–N2′: 2.67 Å, and N1–N2: 2.75 Å, N1–N2′: 2.70 Å respectively).[13a,c] Our attempt to synthesize the Pd^{II}-complex of DNP with $Pd(OAc)_2$ in refluxing acetic acid led to isolation of a green colored complex of palladium, which showed a porphycene-type absorption spectrum, albeit quite broad, with mass 957.1887 (HRMS). The ^1H NMR spectrum of this compound appears to be symmetrical in nature (Supporting Information, Figure S1). However, data could not be fit into any tangible Pd^{II}-complex. Fortunately, single crystals grown from slow evaporation of a $CHCl_3$ solution at room temperature helped us to ascertain the solid state structure by single crystal XRD analysis. It revealed the formation of an unique dipalladium complex **5**, that is, $[Pd_2(\mu\text{-DNP})(\mu\text{-OAc})_2]$, where the porphycene ligand undergoes serious ring deformation and takes a bowl shape geometry (Figure 2). The two metal ions coordinate with opposite ring N-atoms (N1, N2′ and N2, N1′) on the convex side of the bowl, and two bridging acetate ligands satisfy the remaining valences, leading to both palladiums in their formal +2 oxidation states. Average deviation of nitrogen atoms from the mean porphycene plane (excluding the isopropyl substituents) is found in the range of 0.783–0.848 Å above the mean plane, which is almost more than five times higher than that observed in freebase DNP (0.15 Å). The formation of such a stable bimetallic complex with a rigid ligand framework, such as DNP, at the cost of large ring strain is indeed highly remarkable. Interestingly, the Pd–Pd distance was found to be 2.67 Å, which is quite shorter than their van der Waals radii (3.26 Å).[14] The two Pd^{II} units were found to reside 2.219 Å above the porphycene mean plane. Further, an unprecedented complexation induced core expansion was noticed in **5**, with N1-N2′ and N1-N2 distances of 2.687 and 3.106 Å respectively, compared to that observed in the corresponding freebase DNP (2.49 and 2.95 Å).

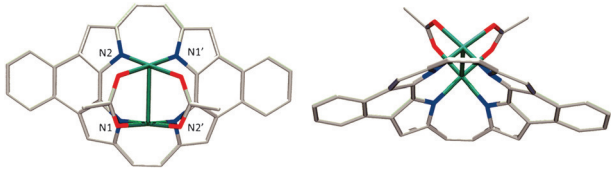

Figure 2. Molecular structure of $[Pd_2(\mu\text{-DNP})(\mu\text{-OAc})_2]$ **5**. Left: Front view. Right: Side view. *iso*-propyl (*i*Pr) groups and H atoms were omitted for clarity. Gray = C, blue = N, red = O, and green = Pd.

The very short Pd–Pd distance observed in the crystal structure led us to investigate possible metal–metal bonding in **5**. To understand the nature of the metal–metal interaction, we performed DFT calculations by taking the crystal structure coordinates as the input file.[15a] Natural bond orbital (NBO) analysis, Wiberg bond index in NAO basis shows the bond order between Pd-Pd is 0.18. The major orbital contributions towards the corresponding bond were found to be 4d (32.14 %) and 5s (4.28 %) orbitals from each Pd atom as calculated by Multiwfn software,[15b] which was clearly visualized from the electron density map of MO 198 (HOMO-17) and the electrostatic potential (esp) array contour plots (Figure 3). Furthermore, topological analysis of electron density according to Bader's quantum theory of atoms in molecules (QTAIM) confirms the presence of bonding interaction between Pd···Pd atoms (Supporting Information, Table S1).[15c]

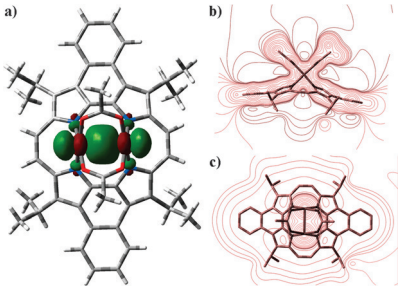

Figure 3. Visualization of bonding interactions with isosurface value (0.04). a) Electron density map of MO 198 (HOMO-17). b) ESP array contour plot at plane formed by Pd, N, and O atoms. c) ESP array contour plot at plane formed between the two Pd atoms in **5**.

The ^1H NMR spectrum of complex **5** measured in $CDCl_3$ now could be unequivocally assigned to the bimetallic complex observed in the crystal structure, where two doublets correspond to the *i*Pr CH_3 protons, in an otherwise symmetric spectrum. This diastereotopicity of the CH_3 signal can be attributed to the bowl shape of the macrocycle.[16] On the other hand, to check the effect of bridging ligand towards the complexation event, we performed the reaction with acac in place of OAc as the metal carrier salt. Refluxing DNP with $Pd(acac)_2$ in *o*-dichlorobenzene and pyridine resulted in an unusual mono-Pd^{II} complex **6** with mass 831.2873.[13a] In this case, the Pd atom likely coordinates with two core nitrogens at one side and one acac ligand on the other side, thereby leaving the remaining two nitrogens uncoordinated. Interestingly, complexation led to reduced symmetry of the macrocycle, as clearly seen in the ^1H NMR spectrum (Supporting Information, Figure S2), and may be attributed to the unsym-

metrical coordination mode of the metal to the porphycene ligand. For example, two clear *meso* signals appeared at 9.50 and 9.40 ppm. Likewise signals corresponding to *i*Pr CH and CH_3 also split into two and four sets of signals, respectively. Furthermore, acac signals were observed at 3.95 ppm (CH) and 0.89 ppm (CH_3), and corresponding integral values clearly indicate the presence of only one acac ligand. The downfield chemical shift of the NH resonance appearing at 8.70 ppm (confirmed by D_2O exchange; Supporting Information, Figure S3), suggests strong NH···N hydrogen bonding as noticed in the case of freebase DNP (9.08 ppm). This type of N1,N2′ coordination mode of the Pd in **6** has no precedence in porphycene chemistry. However, a similar type of complex in the case of porphyrin was first reported by Callot et al. and could only be achieved after *N*,*N*′-protection.[17] Single crystal (grown from slow evaporation of a solution in dichloromethane and acetonitrile mixture) X-ray structural analysis of **6** finally confirmed the N1,N2′ coordination of the Pd ion unequivocally (Figure 4). Interestingly, here the porphycene

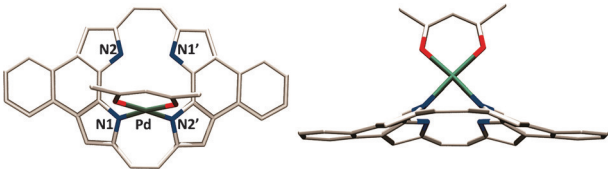

Figure 4. Molecular structure of [Pd(μ-DNP)(μ-acac)] **6**. Left: Front view. Right: Side view. *i*Pr groups and H atoms were omitted for clarity. Gray = C, blue = N, red = O, and green = Pd.

macrocycle acts as a bidentate ligand to coordinate with the Pd on one side and one acac ligand completes the coordination sphere on the other side, thereby leaving the remaining two nitrogen atoms of DNP uncoordinated. Although the crystal structure of [Pd(μ-DNP)(μ-acac)] **6** exhibits a non-planar geometry, the extent of ring distortion is less pronounced compared to that in the dipalladium complex **5**. The two nitrogens involved in complexation were deviated more compared to the free nitrogens (0.679–0.687 Å vs 0.558–0.567 Å), with the Pd ion situated 2.088 Å above the mean plane. Interestingly, N1–N2′ (2.685 Å) and N1–N2 (3.00 Å) distances observed for **6** were also very similar to that in **5**. This clearly indicates complexation with palladium led to core expansion of the porphycene macrocycle. To better understand the preferential coordination modes of Pd to form a seven-membered metalacycle **6** (through N1, N2′ coordination) over the five-membered one **7** (through N1, N2 coordination) in the mono metallic complex (Supporting Information, Table S2), we optimized both the structures using DFT analysis. The optimized structures clearly display the relatively greater stability of the complex **6**, which is 1.46 eV lower in energy compared to that of **7** (Supporting Information, Table S2). We believe the favorable formation of strong NH···N hydrogen bonding in **6** than **7** possibly dictates this preference for the seven-membered cyclometalated species.

The UV/Vis-NIR absorption spectra of the two metalloporphycene complexes **5** and **6** clearly reflect the ring

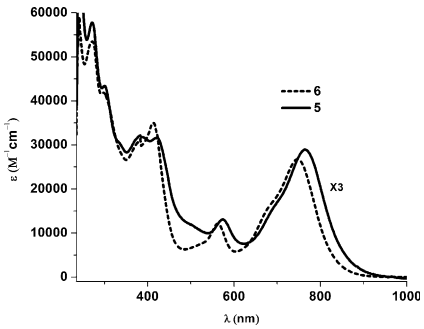

Figure 5. UV/Vis-NIR spectra of Pd-complexes **5** and **6** recorded in $CHCl_3$ at room temperature.

deformation in the macrocycle upon complexation (Figure 5). For example, the dipalladium complex **5** shows a broad split Soret band at 383 and 420 nm with drastically reduced absorption intensity compared to the corresponding Ni^{II}- and Cu^{II}- complexes.[13a,c] Unlike other dinaphthoporphycenes and their metal complexes, where four Q-type bands were observed, here it reduces to two with the higher energy bands almost merging with their corresponding neighboring bands appearing at 574 and 764 nm. Furthermore, the lowest energy Q-band in **5** found to be quite intense (Q-band/Soret band intensity ratio ≈0.93), with large red shifted absorption compared to the freebase (46 nm).[13a] In contrast, the mono-Pd-complex **6** shows more intense absorption bands with at least three-times larger extinction coefficient compared to the dipalladium complex **5**. Complex **6** exhibits a Soret type band at 413 nm with a shoulder at 383 nm along with two Q-bands at 563 and 747 nm. These bands are blue shifted relative to that of complex **5**. The lowest energy Q-band of **6** was found to be relatively less intense than that of complex **5** (Q-band/Soret band intensity ratio 0.77 vs 0.93). These observations clearly indicate that non-planarity in the dipalladium complex is more pronounced compared to the mono-metallic complex.

Electrochemical analyses of both the metallo-derivatives were carried out by cyclic voltammetry (CV) and differential pulse voltammetry (DPV) using tetrabutylammonium hexafluorophosphate as the supporting electrolyte. Both complexes exhibit two reversible one-electron reduction and two one-electron oxidation potentials (Figure 6). Table 1 shows their half-wave potentials along with that of the freebase.[13c] The voltammograms and data clearly reveal the effect of core distortion and resultant symmetry of the macrocycles upon complexation. Comparison of these redox potentials to that of the freebase DNP indicates complexation led to facile oxidation of the macrocycles and more difficult reduction. Furthermore, porphycene ring distortion led to a decrease in

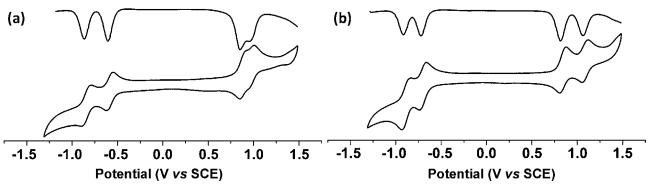

Figure 6. CV (below) and DPV (above) of complexes (a) **5** and (b) **6** in dichloromethane measured at 298 K.

Table 1: Comparative redox potentials (in V vs. SCE) of DNP and its Pd-complexes.

Compound	Oxidation ($E_{1/2}$)	Reduction ($E_{1/2}$)	$\Delta E_{1/2}$
$[Pd_2(\mu\text{-DNP})(\mu\text{-OAc})_2]$, **5**	+0.86,[a] +0.96[a]	−0.58, −0.84	1.44
[Pd(μ-DNP)(μ-acac)], **6**	+0.85, +1.09	−0.69, −0.88	1.54
DNP,[b] **1**	+0.99, +1.36	−0.59, −0.85	1.58

[a] Measured by DPV. [b] As reported in Ref. [13c].

the HOMO–LUMO gap, as can be seen from the $\Delta E_{1/2}$ values (Table 1), with the increasing order **5** < **6** < DNP. In view of the similar redox potentials of the two Pd complexes with that of freebase DNP, it can be concluded that the redox processes are ligand-centered rather than metal-centered.

The large distortion of the planar aromatic DNP ligand in order to complex with Pd led us to explore their aromaticity with the aid of nucleus-independent chemical shift (NICS) values,[18] and harmonic oscillator model of aromaticity (HOMA) indices (Supporting Information, Table S3).[19] The NICS values reveal complexation of DNP (−10.77 ppm) resulted in an enhancement of aromaticity for both the complexes, **5** (−12.75 ppm) and **6** (−11.75 ppm). The HOMA indices also provided the extent of electron delocalization, for DNP (0.326), **5** (0.574), and **6** (0.579), further confirming the complexation induced increase in aromaticity of the Pd-complexes (Supporting Information, Table S3).

In summary, for the first time in porphyrin coordination chemistry, we could realize a cis-bimetallic complex using a rigid isomeric porphyrin platform, that is, dinaphthoporphycene that also exhibits metal–metal bonding interactions. Dipalladium complexes are of great contemporary interest as attractive catalysts for key oxidative transformations in organic synthesis.[20] So far the reported dipalladium complexes are built around ligands which do not communicate between themselves; however, in the present system, the redox active porphycene macrocycle acting as a bidentate ligand to both the metal centers can enhance the redox synergy between them. Moreover, we have also reported another mono-Pd^{II} complex of dinaphthoporphycene, displaying sideways coordination to Pd involving two ring nitrogens only. The unsymmetrical coordination mode and the unique geometry may find application in asymmetric catalysis. Formation of these complexes clearly unravels the possibility of further fine tuning of their structure and electronic properties. Notably, all metalloporphycenes reported so far are mainly inspired by the existing similar metalloporphyrins, while the reverse is not true. These findings will certainly stimulate researchers to re-evaluate the coordination chemistry of porphycene vis-a-vis porphyrin.

Acknowledgements

This work is supported by the Department of Science and Technology (DST), India and Council of Scientific & Industrial Research (CSIR), India through project no. SR/S1/IC-56/2012 and 01/(2449)/10/EMR-II, respectively. Authors thank Center for Modeling, Simulation and Design (CMSD), University of Hyderabad for computational facility. T. S. thanks University Grant Commission (UGC), India for financial assistance under University with Potential for Excellence (UPE2) scheme. B. S. K. thanks CSIR for senior research fellowship. Authors thank Dr. N. Raju, School of Chemistry, University of Hyderabad for his initial efforts in this project and Dr. T. Y. Gopalakrishna, IISER, Pune, India for his inputs in performing NICS & HOMA calculations.

Keywords: aromaticity · bimetallic complexes · dipalladium–complexes · porphycenes · porphyrinoids

How to cite: *Angew. Chem. Int. Ed.* **2015**, *54*, 14835–14839
Angew. Chem. **2015**, *127*, 15048–15052

[1] K. M. Kadish, K. M. Smith, R. Guilard, *The Porphyrin Handbook*, Vol. *3*, Academic Press, San Diego, **2000**.
[2] a) D. Cullen, E. Meyer, T. S. Srivastava, M. Tsutsui, *J. Am. Chem. Soc.* **1972**, *94*, 7603–7605; b) D. Ostfeld, M. Tsutsui, C. P. Hrung, D. C. Conway, *J. Am. Chem. Soc.* **1971**, *93*, 2548–2549.
[3] a) S. Le Gac, L. Fusaro, T. Roisnel, B. Boitrel, *J. Am. Chem. Soc.* **2014**, *136*, 6698–6715; b) B. Najjari, S. Le Gac, T. Roisnel, V. Dorcet, B. Boitrel, *J. Am. Chem. Soc.* **2012**, *134*, 16017–16032; c) N. Motreff, S. Le Gac, M. Luhmer, E. Furet, J.-F. Halet, T. Roisnel, B. Boitrel, *Angew. Chem. Int. Ed.* **2011**, *50*, 1560–1564; *Angew. Chem.* **2011**, *123*, 1598–1602; d) Z. Halime, M. Lachkar, T. Roisnel, E. Furet, J.-F. Halet, B. Boitrel, *Angew. Chem. Int. Ed.* **2007**, *46*, 5120–5124; *Angew. Chem.* **2007**, *119*, 5212–5216.
[4] D. V. Partyka, T. J. Robilotto, M. Zeller, A. D. Hunter, T. G. Gray, *Proc. Natl. Acad. Sci. USA* **2008**, *105*, 14293–14297.
[5] a) E. Vogel, M. Köcher, H. Schmickler, J. Lex, *Angew. Chem. Int. Ed. Engl.* **1986**, *25*, 257–259; *Angew. Chem.* **1986**, *98*, 262–264; b) D. Sánchez-García, J. L. Sessler, *Chem. Soc. Rev.* **2008**, *37*, 215–232.
[6] J. C. Stockert, M. Cañete, A. Juarranz, A. Villanueva, R. W. Horobin, J. I. Borrell, J. Teixidó, S. Nonell, *Curr. Med. Chem.* **2007**, *14*, 997–1026, and references therein.
[7] a) E. Vogel, P. Koch, X.-L. Hou, J. Lex, M. Lausmann, M. Kisters, A. M. Aukauloo, P. Richard, R. Guilard, *Angew. Chem. Int. Ed. Engl.* **1993**, *32*, 1600–1604; *Angew. Chem.* **1993**, *105*, 1670–1673; b) E. Vogel, M. Köcher, J. Lex, O. Enmer, *Isr. J. Chem.* **1989**, *29*, 257–266; c) C. J. Fowler, J. L. Sessler, V. M. Lynch, J. Waluk, A. Gebauer, J. Lex, A. Heger, F. Zuniga-y-Rivero, E. Vogel, *Chem. Eur. J.* **2002**, *8*, 3485–3496.
[8] a) L. Cuesta, E. Karnas, V. M. Lynch, P. Chen, J. Shen, K. M. Kadish, K. Ohkubo, S. Fukuzumi, J. L. Sessler, *J. Am. Chem. Soc.* **2009**, *131*, 13538–13547; b) G. I. Vargas-Zúñiga, V. V. Roznyatovskiy, A. Nepomnyaschii, V. M. Lynch, J. L. Sessler, *J. Porphyrins Phthalocyanines* **2012**, *16*, 479–487; c) L. Cuesta, J. L. Sessler, *Chem. Soc. Rev.* **2009**, *38*, 2716–2729.
[9] T. Kumagai, F. Hanke, S. Gawinkowski, J. Sharp, K. Kotsis, J. Waluk, M. Persson, L. Grill, *Nat. Chem.* **2014**, *6*, 41–46.
[10] C. M. Che, Z. Y. Li, C. X. Guo, K. Y. Wong, S. S. Chern, S. M. Peng, *Inorg. Chem.* **1995**, *34*, 984–987.
[11] D. I. AbuSalim, G. M. Ferrence, T. D. Lash, *J. Am. Chem. Soc.* **2014**, *136*, 6763–6772.
[12] a) E. Vogel, I. Grigat, M. Köcher, J. Lex, *Angew. Chem. Int. Ed. Engl.* **1989**, *28*, 1655–1657; *Angew. Chem.* **1989**, *101*, 1687–1689; b) K. Oohora, A. Ogawa, T. Fukuda, A. Onoda, J.-y. Hasegawa, T. Hayashi, *Angew. Chem. Int. Ed.* **2015**, *54*, 6227–6230; *Angew. Chem.* **2015**, *127*, 6325–6328.
[13] a) T. Sarma, P. K. Panda, P. T. Anusha, S. V. Rao, *Org. Lett.* **2011**, *13*, 188–191; b) V. Roznyatovskiy, V. Lynch, J. L. Sessler, *Org. Lett.* **2010**, *12*, 4424–4427; c) T. Sarma, P. K. Panda, *J. Chem. Sci.* **2015**, *127*, 235–240.
[14] A. Bondi, *J. Phys. Chem.* **1964**, *68*, 441–451.

[15] a) Gaussian 09, (Revision C.01), M. J. Frisch et al. Gaussian, Inc., Wallingford CT, 2010; b) T. Lu, Multiwfn 3.3.7, A Multifunctional Wavefunction Analyzer, School of Chemical and Biological Engineering, University of Science and Technology: Beijing, China, 2013; http://multiwfn.codeplex.com; c) R. F. W. Bader, *Atoms in Molecules: A Quantum Theory*, Oxford University Press, Oxford, **1994**.
[16] T. Sarma, P. K. Panda, *Chem. Eur. J.* **2011**, *17*, 13987 – 13991.
[17] H. J. Callot, J. Fischer, R. Weiss, *J. Am. Chem. Soc.* **1982**, *104*, 1272 – 1276.
[18] Z. Chen, C. S. Wannere, C. Corminboeuf, R. Puchta, P. v. R. Schleyer, *Chem. Rev.* **2005**, *105*, 3842 – 3888.
[19] T. M. Krygowski, M. Cryan'ski, *Chem. Rev.* **2001**, *101*, 1385 – 1419.
[20] a) D. C. Powers, T. Ritter, *Nat. Chem.* **2009**, *1*, 302 – 309; b) D. C. Powers, T. Ritter, *Acc. Chem. Res.* **2012**, *45*, 840 – 850, and references therein.

Received: September 14, 2015
Published online: October 21, 2015

